

International Journal of Innovative Research in Science, Engineering and Technology

(A High Impact Factor, Monthly, Peer Reviewed Journal)

Visit: www.ijirset.com

Vol. 7, Issue 6, June 2018

Modeling and Analysis of a Marine Propeller with Different Location of Rudder

SK.P.Abdul Azeem Basha¹, T.Seshaiah. M.E.(Ph.D)²

M.Tech Student, Department of Mechanical Engineering, QIS College of Engineering & Technology, Ongole.

Andhra Pradesh State, India¹

Associate Professor, Department of Mechanical Engineering, QIS College of Engineering & Technology, Ongole.

Andhra Pradesh State, India²

ABSTRACT: In designing a ship, propulsive efficiency is a parameter which always is tried to be kept as optimum as possible. An investigation in full scale and model scale of a ship including propeller and rudder, regarding the effect of changing rudder position on variation of propeller characteristics has been carried out. SHIPFLOW software was utilized to apply Computational Fluid Dynamic (CFD) techniques in order to compute the flow around the ship hull, propeller and rudder. Lifting line method which is coupled with RANS solver module of SHIPFLOW is used to simulate and also compute the propeller characteristics. Five different longitudinal rudder positions were investigated and compared to each other in order to determine the optimum longitudinal position of rudder. Furthermore, in model scale, for optimum longitudinal rudder position, one different transverse position of rudder was also evaluated. For computing propeller characteristics, SELFPROPULSION command was applied into computations in order to achieve balance between drag and thrust by adjusting the shaftRPM.

Consequently, optimum rudder position was determined based on model scale results which are reasonably accurate compared to full scale computed results. The reason which made full scale computation results over predicted can be described regarding to grid resolution at the aft part of ship hull which is not compatible with propeller grids. This causes inaccurate interpolation between propeller and hull/rudder grids which concludes over predicted results for fullscale.

I. INTRODUCTION

Regarding the environmental concern and increase of fuel price, optimizing the fuel consumption is nowadays an important issue in all industries. In ship industry one way to decrease the fuel consumption is improving the propulsion system of the ship which results higher propulsive efficiency. One of the options to reach this aim is evaluation of different locations of the rudder in order to improve the propulsive efficiency. It would be time consuming and not cost effective to make a model of every rudder location. Computational fluid dynamic is a good solution for this problem, because you can easily do several cost effective test in a proper amount of time. Different rudder positions can be modelled and simulated in order to improve and optimize the design by trying to increase the propulsion efficiency and at the same time decreasing the side effects such as cavitation and loss in maneuverability.

1. Theory

In this part a short description will be given about the propeller/rudder interaction, Schilling rudder, SHIPFLOW software and Lifting line method for analysing the propeller characteristics.

1.1. Propeller theory

International Journal of Innovative Research in Science, Engineering and Technology

(A High Impact Factor, Monthly, Peer Reviewed Journal)

Visit: www.ijirset.com

Vol. 7, Issue 6, June 2018

To propel ships, a propulsor which can be called propeller is needed. The aim is to create required thrust T for moving ship at a specific speed V and overcoming the resistance R_T which is applied from water to the ship body.

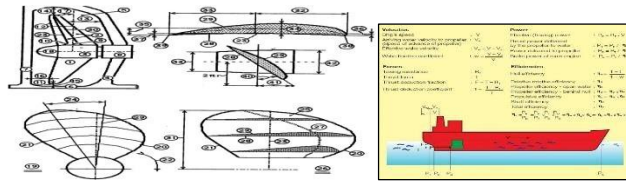


Figure 1. Source:[1]

Figure: Some relevant definitions

Furthermore, as it is shown in Figure 3, the streams coming out of the propeller get blocked and diverted by the rudder which results in decreasing the total axial and tangential velocity. Thrust and torque will therefore be partly higher when a rudder is included. Consequently higher propulsive efficiency might be obtained from propeller/rudder combination as a propulsion system [2].

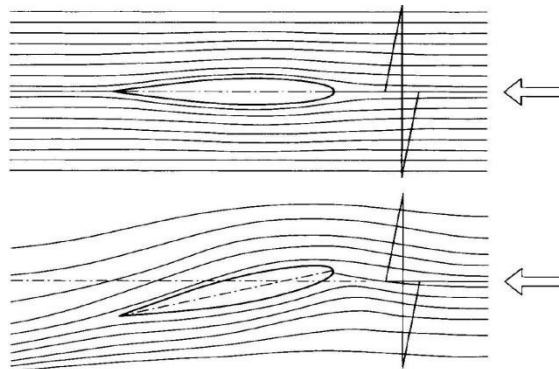


Figure. Blocked and diverted flow by rudder

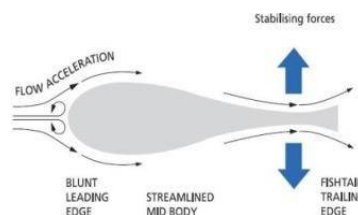


Figure. Schilling rudder cross section, source: www.becker-marine-systems.com

XPAN is the potential flow solver module in SHIPFLOW which computes the flow around 3D objects by using surface singularity panel method. The characteristics which can be computed by XPAN are:

International Journal of Innovative Research in Science, Engineering and Technology

(A High Impact Factor, Monthly, Peer Reviewed Journal)

Visit: www.ijirset.com

Vol. 7, Issue 6, June 2018

XGRID generates grids for computing the turbulent flow which is obtained by solving RANS equations.

XCHAP is executed to solve the RANS equations based on finite volume code. This module which can be applied in zonal and global approach uses different turbulent models such as EASM, k-w BSL and k-w SST. When the zonal approach is used, the boundary condition values for executing XCHAP module are taken from XPAN and XBOUND computation results. Parameters which are computed by XCHAP are:

XCHAP can also be executed on imported structured grids to SHPFLOW [3].

II. GEOMETRY, MESH AND WORK PROCEDURE

2.1. Geometry

Computations in this study are applied on a set of three different geometries. These geometries are, a Ro-Ro ship hull, a FP propeller and a Schillingrudder.

Table 1. Main particulars of the ship

Length LPP [m]	190
Length LWL [m]	223
Draft [m]	10
Beam [m]	32.26

Approximate ship hull geometry data was given by Wallenius Marine AB and represents a typical Ro-Ro vessel. In order to get a good quality of generated mesh, additional offset lines have to be created along the ship hull length. Also increasing the density of offsets in fore and aft part of the ship will help to create higher quality mesh for these curvature shape areas. To reach this aim, an IGES file of ship geometry which is seen in Figure 8 was created by importing the existing offset file of ship hull into RHINO software. A higher quality offset file was made out of this IGES file by help of SHIPFLOW. Some data about ship hull geometry is shown in Table1.

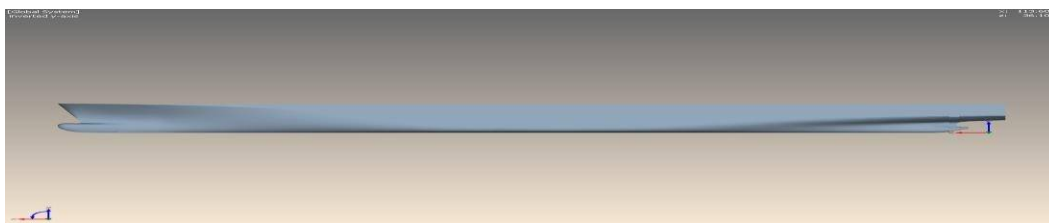


Figure 8. Created ship hull out of primary offset lines

Propeller geometry and its position are specified by a command. The propeller is modelled as an actuator disk in CFD simulation by SHIPFLOW software. Some propeller data is shown in Table 2.

International Journal of Innovative Research in Science, Engineering and Technology

(A High Impact Factor, Monthly, Peer Reviewed Journal)

Visit: www.ijirset.com

Vol. 7, Issue 6, June 2018

Table 2. Some of the propeller's data

Propeller diameter	6800 mm
Hub diameter	1020 mm
Number of blades	4
Rate of revolution	110 rpm

Schilling rudder geometry which is seen in Figure 9 was received as an IGES file. Then a domain was created around the rudder by RHINO software and finally rudder and domain grids were imported as an external mesh into SHIPFLOW for computations.



Figure 9. Schilling rudder geometry

2.2. Grids

In this project, grids were made in two different software. Mesh on the ship hull, free surface and propeller were made in SHIPFLOW. As mentioned before for potential flow calculations, required mesh was generated by XMESH module and for RANS calculations, grids were created by XGRID module. Figure 10 shows generated mesh on ship hull body and free surface.

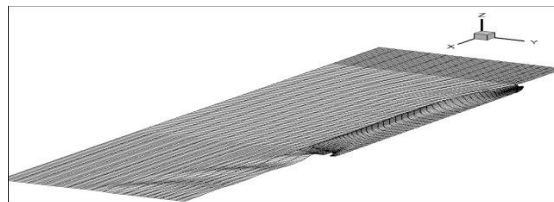


Figure 10. Generated mesh on ship hull body and free surface. SHIPFLOW has the ability to model the rudder geometry by writing a specific command by

which the rudder geometry data is imported into the computations. In order to have the exact rudder geometry it was preferred to make the mesh on the rudder by mesh generator software and then the created rudder mesh was imported into SHIPFLOW as an external mesh. The imported grid should be structured and in Plot3D format file. The rudder/domain mesh was created in GAMBIT software. GAMBIT is not able to export the mesh in Plot3D format, therefore GAMBIT mesh was translated to Plot3D format in ANSYS ICEM CFD software.

International Journal of Innovative Research in Science, Engineering and Technology

(A High Impact Factor, Monthly, Peer Reviewed Journal)

Visit: www.ijirset.com

Vol. 7, Issue 6, June 2018

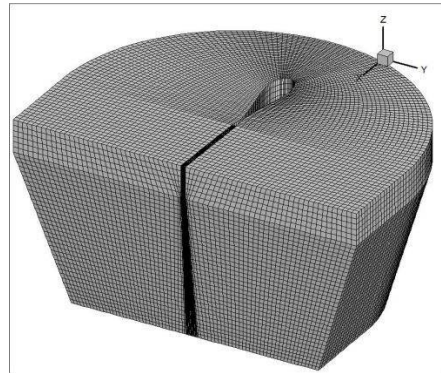


Figure 11. Grids of rudder and domain around the rudder in Plot3D format

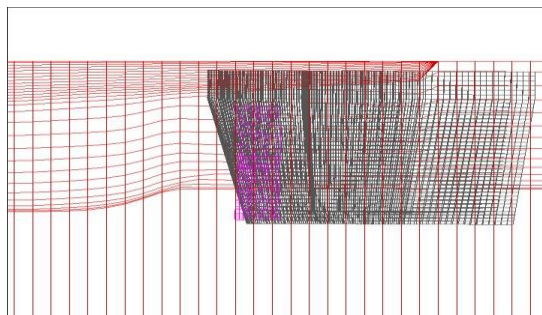


Figure 12. Overlapping grids

Work Procedure

In order to have a good comparison on computed results, computations have been done both in full scale and modelscale.

Five different longitudinal locations of rudder in full scale and model scale have been investigated to come up with the best longitudinal position of the rudder. Also in model scale, for the optimum longitudinal position of rudder regarding the required delivered power, one altered transverse rudder position was also evaluated.

International Journal of Innovative Research in Science, Engineering and Technology

(A High Impact Factor, Monthly, Peer Reviewed Journal)

Visit: www.ijirset.com

Vol. 7, Issue 6, June 2018

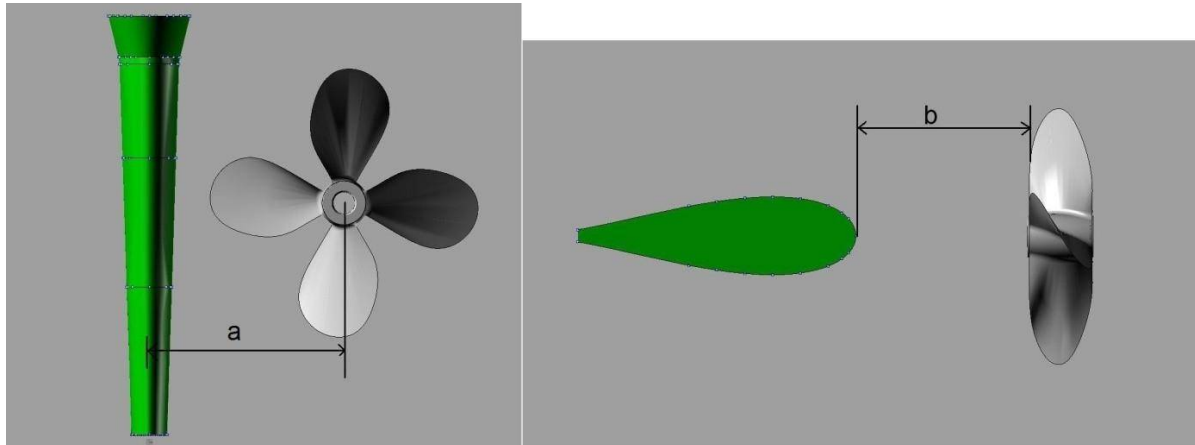


Figure 13. Definition of gap ratio and distance ratio

Some parameters, ratios and defined values regarding these parameters which were used in the computations are defined as:

- = gap ratio, value used = 0.1
- = distance ratio, values used = 0.24, 0.2, 0.17, 0.15, 0.1
- = gap shown in Figure 13
- = distance shown in Figure 13
- D = diameter of propeller
- R = radius of propeller

III. COMPARISON OF THE RESULTS

After running computations for five different longitudinal rudder positions from propeller in full scale and model scale and one transverse rudder position at = 0.1 from propeller in model scale, results are compared to each other as diagrams and tables. At the first step, experimental results and predicted results are compared to calculated results for model scale and full scale respectively. At next step, for model scale and full scale, variation of thrust T, total resistance coefficient Δ and delivered power \dot{W} in different rudder positions are investigated in order to determine the optimum rudder position. Flow fields of different positions are also compared to each other. Table 3 shows some of the necessary results of computed self-propulsion test for ship model scale normalized by experimental values. By comparing the magnitude of obtained torque from computations and measured torque, it is seen that computed torque is around 1.4 % lower than the measured one. Also computed thrust is close to reported thrust from experiment which is 2.2 % lower than the measured one. The difference between computed bare hull resistance and measured bare hull resistance is higher compared to thrust and torque. In this case despite thrust and torque, computed resistance is around 13% higher than the measured one.

Table 3. Experimental data VS computed data for model scale at rudder position = 0.24

	Ship Speed V_s	Model Speed V_m	Torque Q	Thrust T	Resistance $\frac{R}{Tm}$	Rate of revs nm
Computed Data	1	1	0.986	0.978	1.135	1.032

International Journal of Innovative Research in Science, Engineering and Technology

(A High Impact Factor, Monthly, Peer Reviewed Journal)

Visit: www.ijirset.com

Vol. 7, Issue 6, June 2018

Figure 14 shows axial velocity contours at propeller plane for ship model bare hull. Computed results which are in the left side illustrate an acceptable agreement with test results which are shown in the right side.

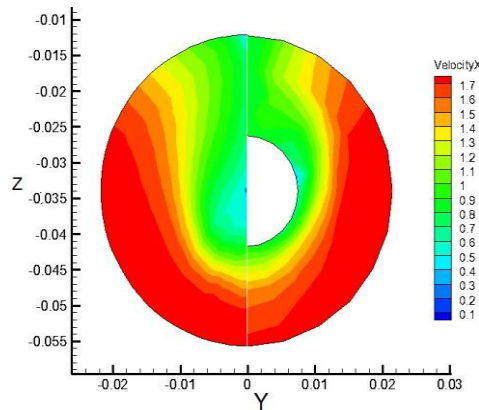


Figure 14. Velocity contours for bare hull at propeller plan, the calculated to left and the measured to the right

Table 4 presents some of the data obtained from CFD computations for full scale normalized by experimentally extrapolated data for full scale according to ITTC 1978 method and also similar.

Table 4. Predicted data according to ITTC1978 method VS computed data for full scale at rudder position

$$bD=0.24$$

	Ship Speed V_s	Effective power P_E	Delivered power P_D	Shaft rate ns	Torque Q	Thrust T	Total Efficiency
Computed Data	1	1.345	1.200	1.090	1.101	1.168	1.108

Among all tested rudder positions for full scale, K_t gets the highest value at position = 0.2. On the other hand lowest value of K_t is specified to the position = 0.2 for model scale.

¹ Björn Regnström, developer of the overlapping grid RANS solver XCHAP at the company Flowtech International AB.

Figure 15. Computed K_Q for full scale and model in different longitudinal rudder positions

As it is observed in Table 5, the highest value for J which means lowest RPM is allocated to position = 0.1. However K_t is not minimum at = 0.1 but regarding to the equations 14 and 7, it is seen that the effect of RPM is two and three times more than K_t on the magnitude of torque Q and delivered power!

International Journal of Innovative Research in Science, Engineering and Technology

(A High Impact Factor, Monthly, Peer Reviewed Journal)

Visit: www.ijirset.com

Vol. 7, Issue 6, June 2018

respectively. So at position=0.1 lowest quantities for Q and P_D were obtained from calculations. Improvement of P_D at position = 0.1 compare to original rudder position at $b/D = 0.24$ was 5.6 %. Location $b/D = 0.2$ is considered as a position among five different defined rudder positions which maximum power is delivered to the shaft to propel the ship with the speed of 20 knots. Calculated P_D at this point is around 4.43% more than P_D of original position of rudder.

$$P_D = 2\pi n^3 K_Q \tag{14}$$

Table 5. Computed data for full scale

b/D	J	K_Q	Q [kN.m]	P_D [MW]
0.24	0.800642	0.0286366	1524.14	18.097
0.2	0.797677	0.0296086	1587.6	18.92
0.17	0.809642	0.0286072	1488.9	17.48
0.15	0.803064	0.0287147	1519.09	17.98
0.1	0.818986	0.0289217	1471.13	17.076

Produced thrust by propeller is calculated according to equation 15. Regarding the tabulated data for full scale in Table 7 and drawn diagram in Figure 21, it is seen, at rudder position $b/D = 0.2/J$ has the lowest value among five different rudder positions which means RPM is the highest, plus K_Q has also the highest value in that location which ends up to give the highest magnitude for thrust T. Calculated thrust at this position is around 4.3 % more than calculated thrust at original rudder position.

$$T = K_T n^5 \tag{15}$$

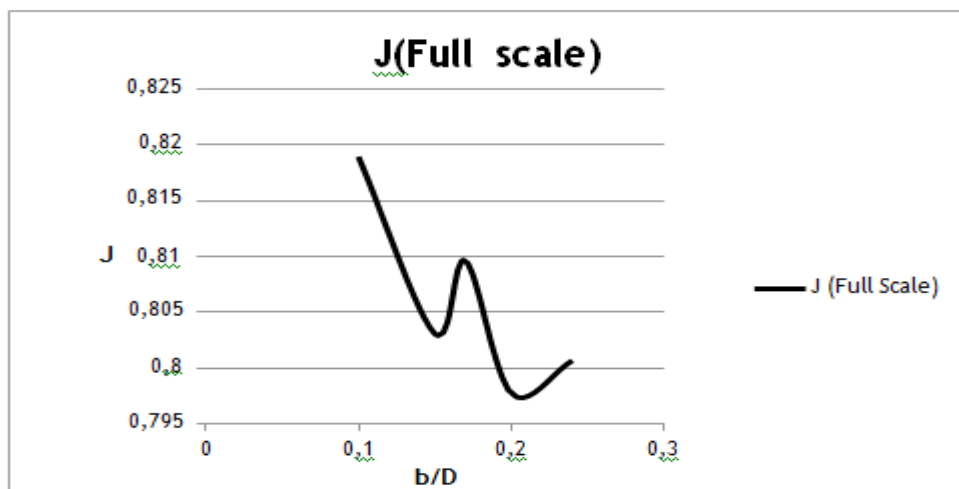


Figure 16. Variation of J at different rudder positions in full scale

International Journal of Innovative Research in Science, Engineering and Technology

(A High Impact Factor, Monthly, Peer Reviewed Journal)

Visit: www.ijirset.com

Vol. 7, Issue 6, June 2018

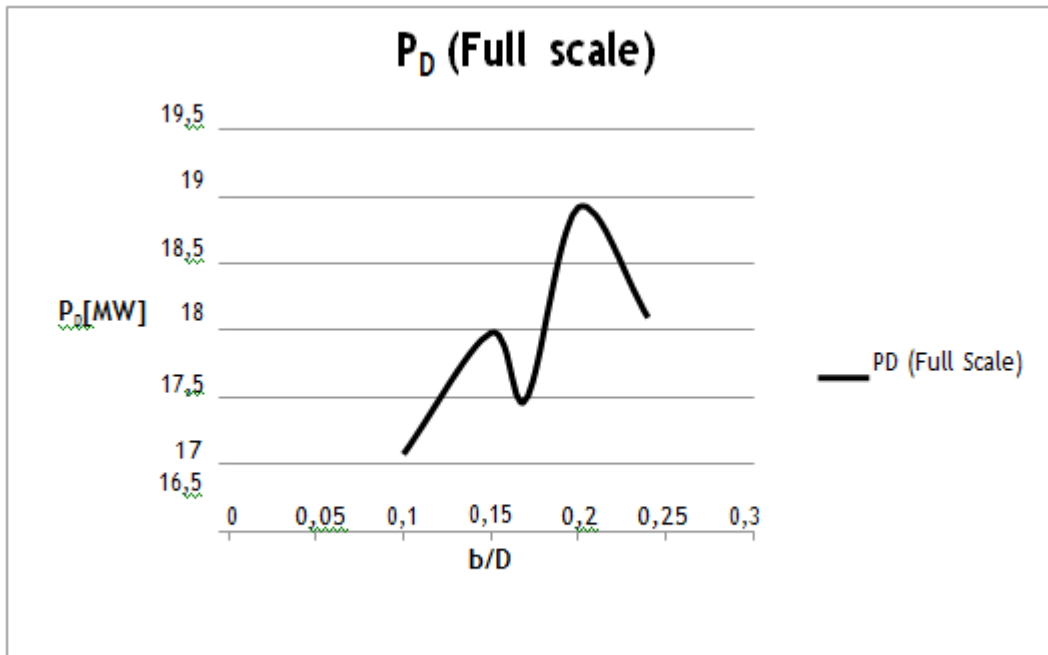


Figure 17. Variation of PD at different rudder positions in full scale.

Table 6. Computed data for model scale

b/D	J	K_q	Q [N.cm]	P_D [W]
0.24	0.845622	0.0310945	189.39	112.1
0.2	0.871167	0.0308964	177.31	104.94
0.17	0.853241	0.0310949	186.02	110.1
0.15	0.849705	0.0310552	187.33	110.87
0.1	0.854722	0.0312058	186.04	110.11

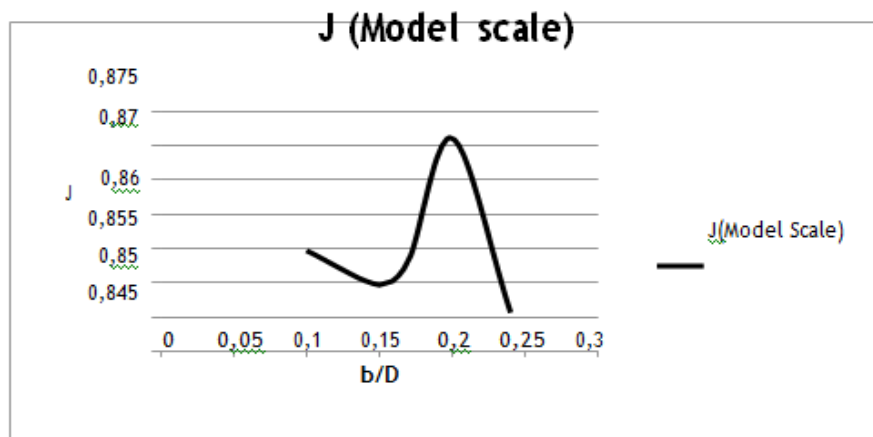


Figure 18. Variation of J at different rudder positions in model scale

International Journal of Innovative Research in Science, Engineering and Technology

(A High Impact Factor, Monthly, Peer Reviewed Journal)

Visit: www.ijirset.com

Vol. 7, Issue 6, June 2018

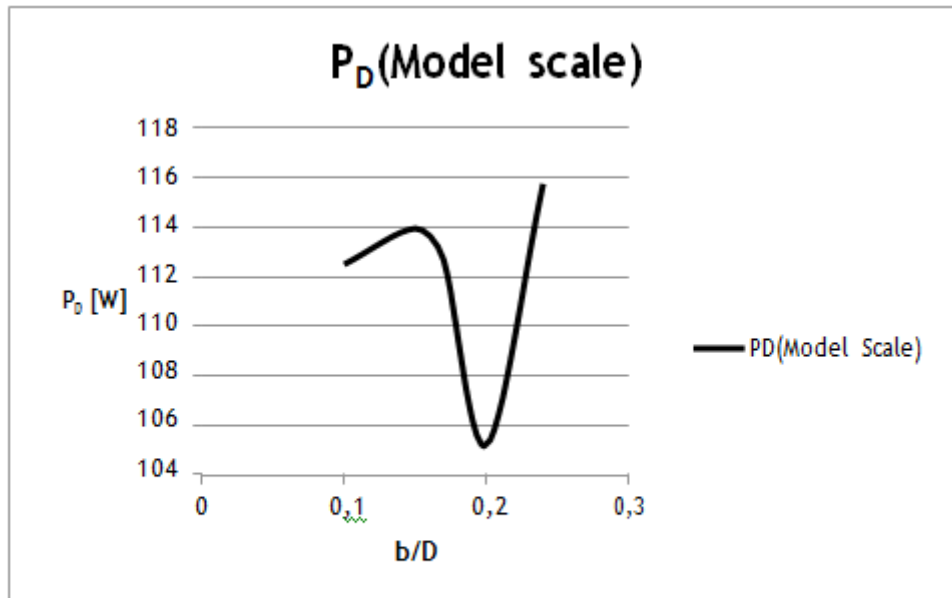


Figure 19. Variation of P_D at different rudder positions in model scale

4.3. Thrust coefficient K_t /thrust T in different rudder positions

K_t is also one of the other output results of SHIPFLOW computations for propeller which is called thrust coefficient. Computed results of K_t for model scale and full scale have been shown in Figure 20.

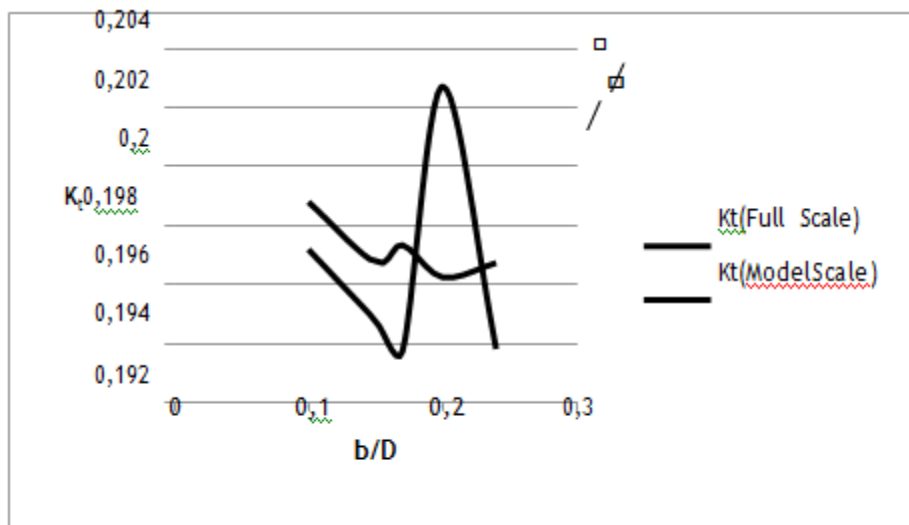


Figure 20. Computed K_t for full scale and model in different longitudinal rudder positions

International Journal of Innovative Research in Science, Engineering and Technology

(A High Impact Factor, Monthly, Peer Reviewed Journal)

Visit: www.ijirset.com

Vol. 7, Issue 6, June 2018

Produced thrust by propeller is calculated according to equation 15. Regarding the tabulated data for full scale in Table 7 and drawn diagram in Figure 21, it is seen, at rudder position

$= 0.2/J$ has the lowest value among five different rudder positions which means RPM is the highest, plus K_t has also the highest value in that location which ends up to give the highest magnitude for thrust T . Calculated thrust at this position is around 4.3 % more than calculated thrust at original rudder position.

$$= K_t n^3 \tag{15}$$

Table 7. Calculated data for full scale

b/D	J	K_t	T (kN)
0.24	0.800642	0.193828	1277.245
0.2	0.797677	0.202719	1335.833
0.17	0.809642	0.193741	1276.671
0.15	0.803064	0.194783	1283.538
0.1	0.818986	0.197196	1299.438

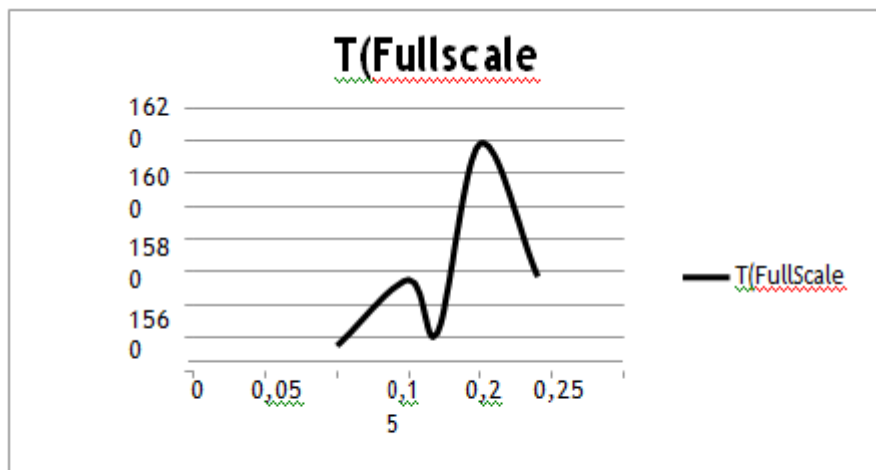


Figure 21. Variation of T at different rudder positions in full scale

In model scale by evaluating tabulated data in Table 8, it is observed that at the position $= 0.1$, K_t has the highest value. On the other hand at position $= 0.24$ which is the original position of the rudder J value is the lowest and therefore RPM is the highest among all tested

positions. Consequently highest thrust is produced at $= 0.24$ by the propeller. Lowest produced thrust is allocated to rudder position $= 0.2$ which is around 6.5 % less than maximum produced thrust at $= 0.24$.

International Journal of Innovative Research in Science, Engineering and Technology

(A High Impact Factor, Monthly, Peer Reviewed Journal)

Visit: www.ijirset.com

Vol. 7, Issue 6, June 2018

Table 8. Calculated data for model scale

b/D	J	K_t	T [N]
0.24	0.845622	0.196733	52.1
0.2	0.871167	0.196247	48.96
0.17	0.853241	0.197345	51.33
0.15	0.849705	0.19675	51.6
0.1	0.854722	0.198804	51.53

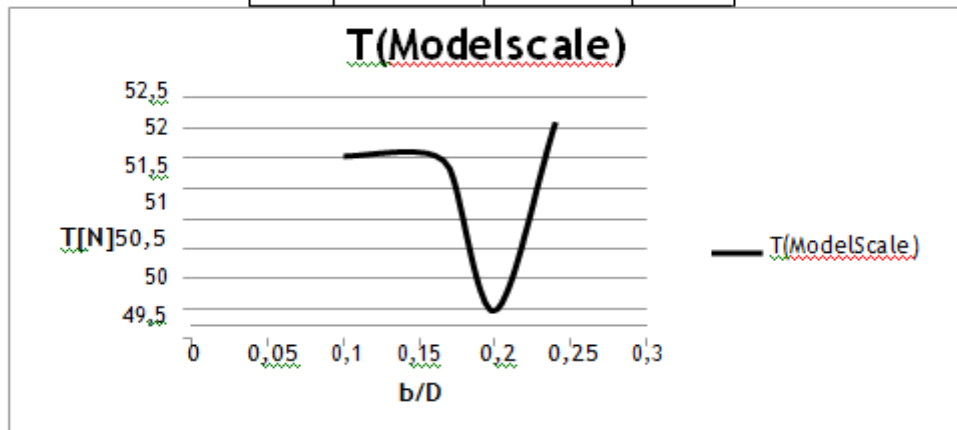


Figure 22. Variation of T at different rudder positions in model scale

4.4. Total resistance coefficient C_t in different rudder positions

For calculating total resistance coefficient C_t , wave resistance was also included into total resistance coefficient computations.

$$C_t = C_{Dp} + C_{Dw}$$

$$C_t = C_{Dp} + C_{Dw}$$

Table 9. Computed total resistance coefficient in full scale and model scale

b/D	C_t (Full Scale)		C_t (Model Scale)
	Hull + Propeller + Append	Hull + Append	Hull + Propeller + Append
0.24	3.54E-03	3.13E-03	4.65E-03
0.2	3.35E-03	3.01E-03	4.47E-03
0.17	3.47E-03	3.07E-03	4.60E-03
0.15	3.53E-03	3.14E-03	4.62E-03
0.1	3.46E-03	3.06E-03	4.60E-03

International Journal of Innovative Research in Science, Engineering and Technology

(A High Impact Factor, Monthly, Peer Reviewed Journal)

Visit: www.ijirset.com

Vol. 7, Issue 6, June 2018

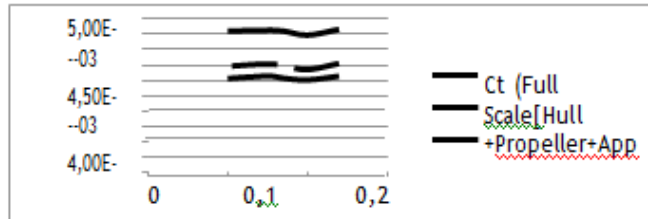


Figure 23. Variation of total resistance coefficient C_t in full scale and model scale

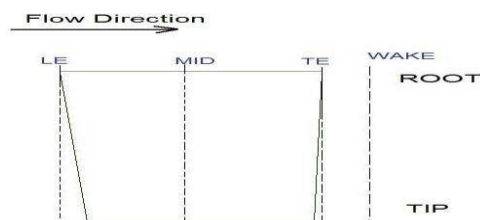
Table 10. Comparison between two different transverse positions

L/R	K_r	K_t	Shaft rate ns [1/s]	Torque Q [N.cm]	Thrust T [N]	Delivered power P_D [W]	C_t
0	0.0308	0.19624	9.44	177.3	48.96	105.19	0.004465
0.1	0.0275	0.16792	8.4	125.1	33.15	66.03	0.00435

4.5. Flow field

In order to study the effect of different rudder positions on the flow around the rudder, axial velocity contours were computed and investigated for model scale, for four different positions along the rudder. As it is shown in Figure 24, they are located at leading edge, middle of the rudder, trailing edge and behind the trailing edge.

Figure 24. Four different positions along the rudder



International Journal of Innovative Research in Science, Engineering and Technology

(A High Impact Factor, Monthly, Peer Reviewed Journal)

Visit: www.ijirset.com

Vol. 7, Issue 6, June 2018

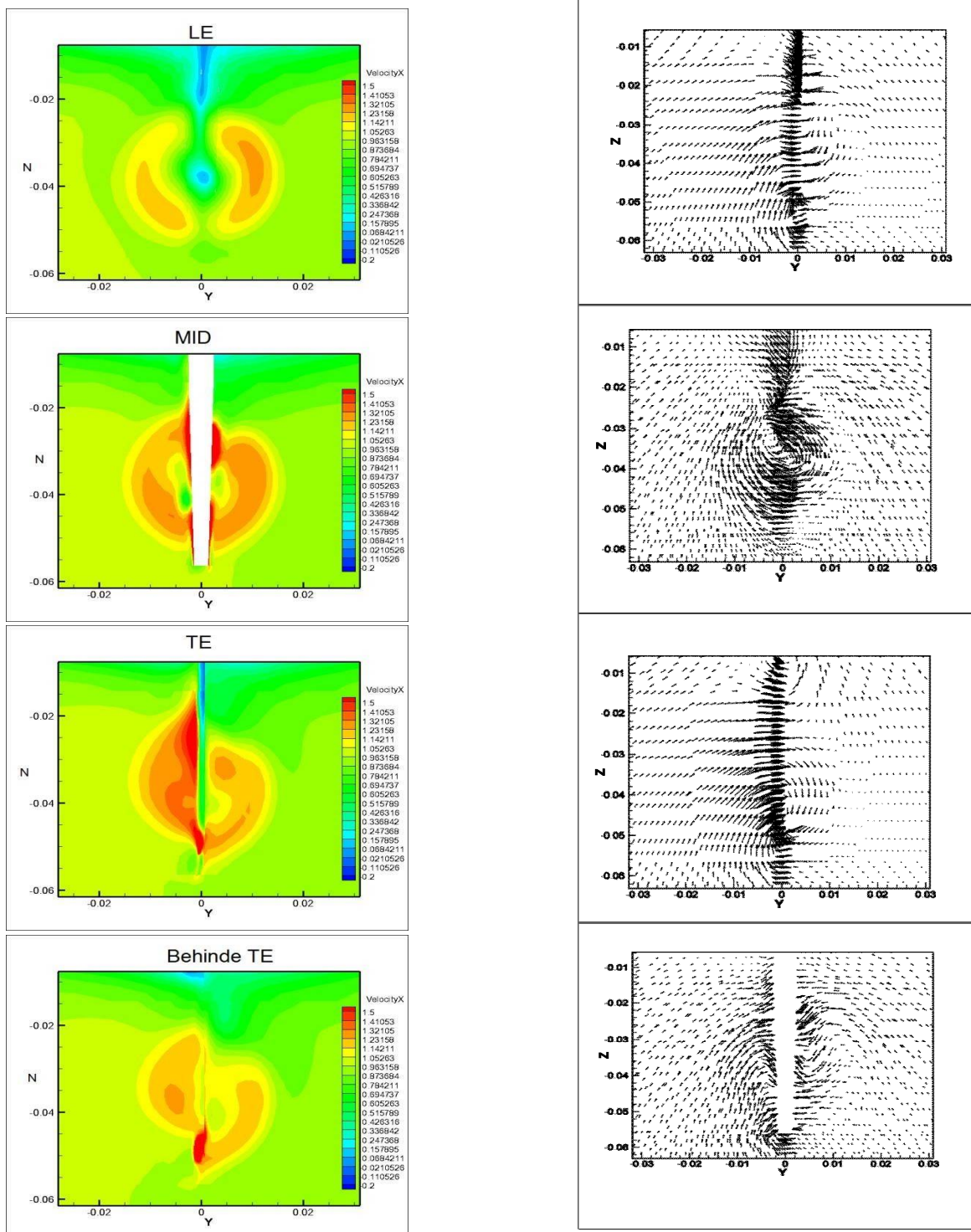


Figure 25. Axial velocity contours and crossflow vectors across along the rudder at rudder position = 0.24

International Journal of Innovative Research in Science, Engineering and Technology

(A High Impact Factor, Monthly, Peer Reviewed Journal)

Visit: www.ijirset.com

Vol. 7, Issue 6, June 2018

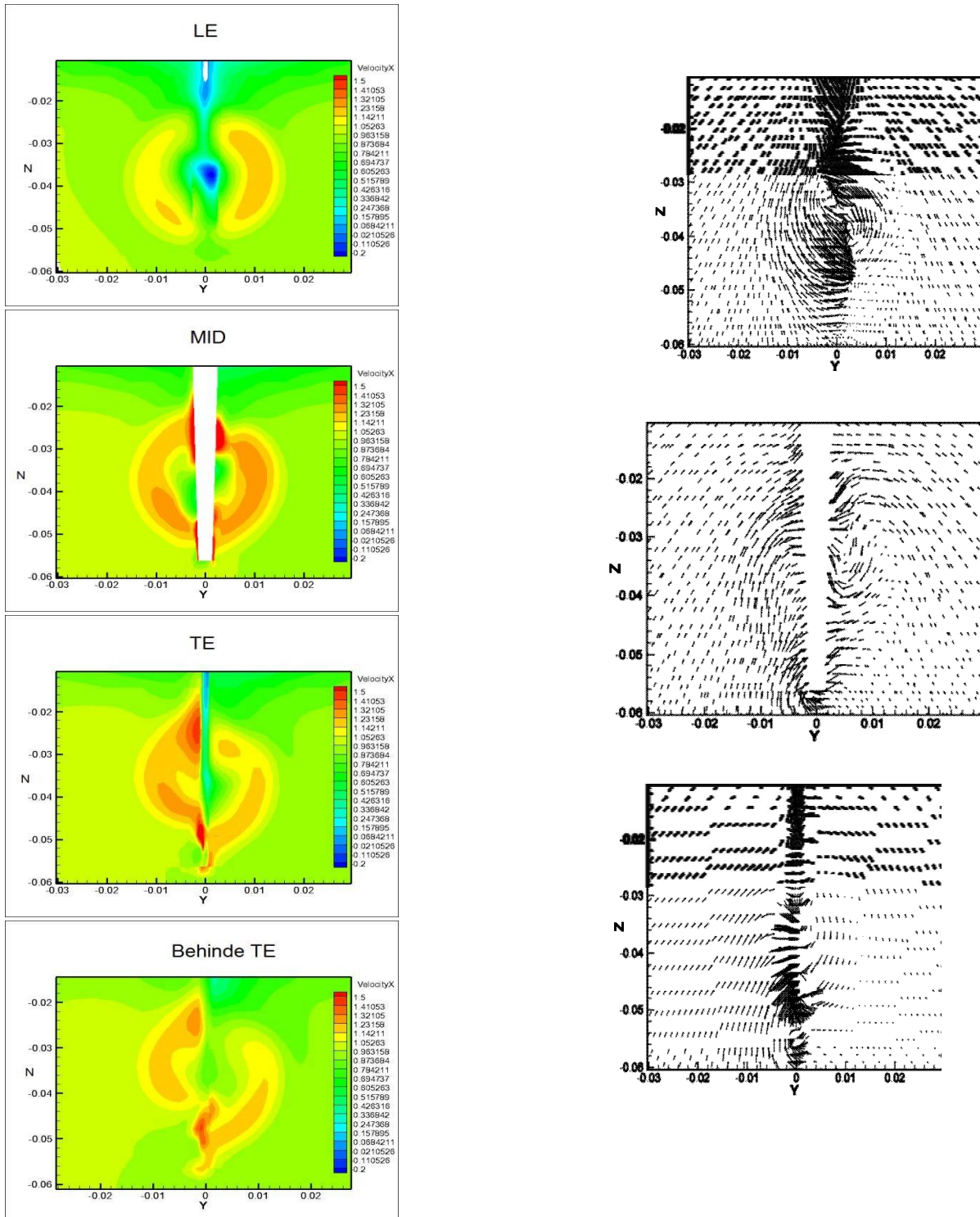


Figure 25. Axial velocity contours and crossflow vectors across along the rudder at mod elscaler related to rudder position = 0.24

International Journal of Innovative Research in Science, Engineering and Technology

(A High Impact Factor, Monthly, Peer Reviewed Journal)

Visit: www.ijirset.com

Vol. 7, Issue 6, June 2018

4.6. Pressure distribution on ruddersurface

The pressure distribution on the surface of the rudder for different rudder positions is shown in Figure 31 to Figure 36. The images in the left side represent the pressure side of the rudder and the right images show the suction side of the rudder for all rudderpositions.

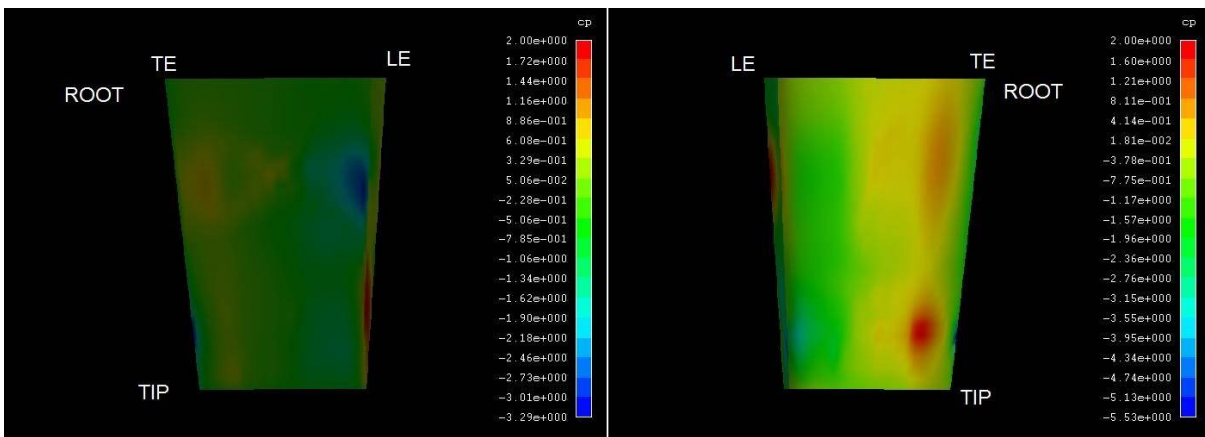


Figure31. Pressuredistributiononpressureside(leftimage)andsuctionside(rightimage) oftherudderat position= 0.24

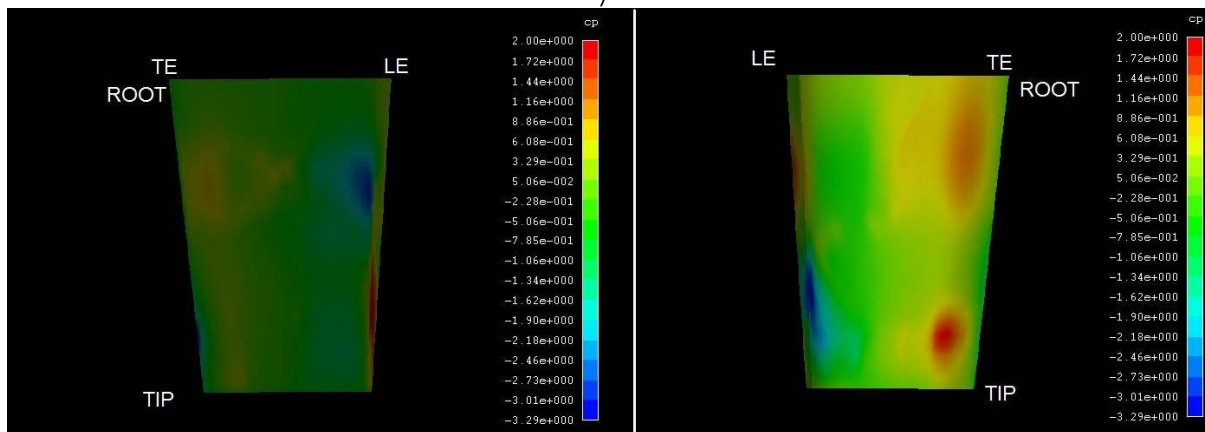


Figure32. Pressuredistributiononpressureside(leftimage)andsuctionside(rightimage) oftherudderat position= 0.2

V. DISCUSSION AND CONCLUSIONS

Regarding to varying the rudder position in order to determine less required delivered power to propel the ship in a specific speed for model scale and corresponding of that speed in full scale, two different rudder positions were determined based on computation results. For model scale, optimum rudder location regarding to delivered power was determined at $b/D = 0.2$, while in full scale it was determined at $b/D = 0.1$. Different optimum rudder positions in model scale and full scale are doubtful. Other questionable results can be referred to computed total resistance coefficient for full scale. As it was seen in Figure 17, Figure 21 and Figure 23, fluctuation of total resistance

International Journal of Innovative Research in Science, Engineering and Technology

(A High Impact Factor, Monthly, Peer Reviewed Journal)

Visit: www.ijirset.com

Vol. 7, Issue 6, June 2018

coefficient C_l for full scale does not agree with the fluctuation of torque and thrust. For example at position = 0.2, C_l is minimum, where the magnitudes of torque Q and thrust T are expected to be minimum as well, but they are not. While C_l fluctuation in different rudder positions in model scale completely agrees with torque and thrust fluctuations.

REFERENCES

- [1] Bark, G. and Dyne, G., 2005, Ship propulsion MMA 155, Department of Shipping and Marine Technology, Chalmers University of Technology, Göteborg.
- [2] Da-Qing Li, 1994, Investigation on Propeller-Rudder Interaction by numerical Methods, Department of Shipping and Marine Technology, Chalmers University of Technology, Göteborg.
- [3] SHIPFLOW 4.3 Users Manual, 2010, Flowtech International AB, Göteborg.
- [4] K.KAFALI, 1961, Propeller characteristics with different locations of the rudders in the propeller race of twin rudders-twin screws ships, Journal of the American Society for Naval Engineers, Vol.73, Issue 2, pp. 369–376, May 1961
- [5] KAI-JIA HAN, 2008, Numerical optimization of hull/propeller/rudder configurations, Department of Shipping and Marine Technology, Chalmers University of Technology, Göteborg.
- [6] Larsson, L. and Raven, H. C., 2004, MMA 155 Ship Resistance and Flow, Göteborg and Wageningen, Chalmers University of Technology.
- [7] K. J. Rawson, E. C. Tupper, 2001, Basic Ship Theory, vol.2, 5th ed, p.385. www.manbw.com/files/news/files/3859/P254-04-04.pdf